SURFACE DISCONTINUITY MODELLING BY LSM THROUGH PATCH ADAPTATION AND USE OF EDGES

M. Pateraki[*], E. Baltsavias

Institute of Geodesy and Photogrammetry, ETH-Hoenggerberg, CH-8093, Zurich, Switzerland
(maria, manos)@geod.baug.ethz.ch

Commission III, WG III/6

KEY WORDS: edges, least squares matching, modelling, discontinuities, reliability, DSM, algorithm, evaluation

ABSTRACT:

This paper handles the aspect of least squares matching (LSM) for DSM generation and focuses mainly on the exploitation of edge information in the least squares approach. The mathematical model of LSM employs an affine transformation to model geometrical distortions between the template and the search images. However, the model, when used for single points that lie close or on edges does not suffice to model discontinuities, especially when patch size is large. To alleviate the above-mentioned problem, LSM is firstly extended to edgels using an approximation of the rotation between search image and template, computed from a signal analysis. The signal analysis is performed by computing the signal ellipses from the template and patch grey levels. Furthermore, the template patch can be pre-rotated and its dimensions can be adjusted, so that the patch becomes a thin ribbon along the edge. Secondly, the model is extended to edge features with topological attributes (edges and vertices with link information). The patch size is adapted to include a whole edge and a non-uniform weighting scheme is utilised in the normal equations of LSM, giving a very low weight to all pixels outside the given edge. After matching the edge middle points, the edge is divided in two segments and the procedure is repeated until the edge segments fall below a certain length threshold. The final stage is the matching of the edge end points, where other edges having the same end point are also taken into account. The proposed techniques are compared to each other and to standard LSM. An evaluation of the methods is done with ADS40 imagery. As it is shown, they lead to less discontinuity smoothing and increase of the success rate and accuracy.

1. INTRODUCTION

Least squares matching (LSM) is one of the key techniques in digital photogrammetry applied to solve feature extraction and correspondence problems as well as surface registration issues by means of least squares adjustment. The LSM method has been addressed by Foerstner (1982) and Ackermann (1984), as a generalization of cross-correlation. Several approaches have been further investigated, employing different radiometric and geometric models for surface reconstruction. Gruen (1985) utilized affine transformation for local surface patch matching assuming that the local surface patch is a plane in sufficient approximation. Gruen and Baltsavias (1988) and Baltsavias (1991) present several aspects regarding the extension of LSM to more than two images and the use of geometric constraints. This approach was later extended to linear CCD satellite images with quasi-epipolar geometry and possibly severe multitemporal differences (Baltsavias and Stallmann, 1992). Rosenholm (1987) employed bilinear finite elements to represent the true surface in multi-point matching, and formulated extensions to include breaklines and surface discontinuities (Rosenholm, 1986) but without performing any investigations. Li (1989) used multi-point matching in a multiresolution, multigrid approach and presented methods for the detection and localisation of breaklines, however with breakline assumptions that are unrealistic, especially for natural scenes. The object-space least squares matching method (Helava, 1988; Wrobel, 1991; Ebner and Heipke, 1988) has been introduced to relate information from images directly to an object space model by including height-, optical-, density-, sensor- and illumination model parameters. The model, however, proved to be computationally expensive and complex as more parameters have to be estimated, and is thus also less stable. LSM has been extended also for edge tracking and matching (Gruen and Stallmann, 1992; Tseng and Schenk,

1992; Gruen and Agouris, 1994), applied to warped images for surface reconstruction (Schenk et al., 1990) and tie point extraction (Krupnik and Schenk, 1997).

LSM is considered to be one of the most precise among existing algorithms (sub-pixel accuracy in the range of 0.01-0.05 pixels for ideal targets and without noise), but it is sensitive to large radiometric differences, is computationally expensive compared to cross-correlation, can not model excessive geometric differences, convergence problems (oscillations, false solutions) may arise if the data have insufficient signal content or if the initial approximations in the least squares solution are not close to the real solution, and, most importantly in the context of this paper, the usual LSM implementation uses area patches and thus smooths surface discontinuities. The focus in this paper is the discontinuity modeling as part of DSM extraction through the exploitation of edge information in LSM. Geometrical constraints are included in the model to reduce search space from 2D to 1D. Various modifications of LSM are presented, as well as experimental results using ADS40 images and manually selected typical discontinuity cases with various problems (e.g. outlines of building roofs) and a comparison to standard LSM.

2. DISCONTINUITY MODELING WITH MODIFIED LSM

2.1 General Estimation Model of LSM

Assume that a surface is viewed in i=0, ..n images of different viewpoints. The problem statement is finding the corresponding

---

part of the template image patch *f(x,y)* in the search images $g_i(x,y)$, i=1,... n, called patches hereafter.

$$f(x, y) - e_i(x, y) = g_i(x, y) \qquad (1)$$

Eq. (1) gives the least squares grey level observation equations, which relate *f(x,y)* and *g$_i$(x,y)* image functions or image patches. The true error vector *e$_i$(x,y)* is included to model errors that arise from radiometric and geometric differences in the images. For the selection of the geometrical model it is assumed that the object surface is approximated by connected local planar facets and the image patches *f(x,y), g$_i$(x,y)* are selected very small with respect to the image size. Therefore, a projective transformation, can be approximated by an affine transformation (Gruen, 1985). Radiometric parameters are not included in the estimation model, instead radiometric corrections are applied prior to (or some of them during) the LSM. These include noise reduction, contrast and edge enhancement and radiometric equalisation among the images.

Geometrical constraints have been proved to strengthen matching in terms of precision and reliability (Baltsavias, 1991) and can be included in the model when information about the sensor orientation model is available. Constraints are employed in the algorithm as additional weighted observation equations. In order to make constraints effective, a very large weight, small standard deviation (s = 0.001 pixel) respectively, must be used (Baltsavias, 1991). The least square solution of the joint system is given by Eq. (2):

$$x = (A^T P A + B^T P_t B)^{-1} (A^T P l + B^T P_t t) \qquad (2)$$

where x is the vector of unknowns, A and B are the design matrices of grey level and geometric constraints observation equations respectively, P and P$_t$ are the respective weight matrices and l and t the discrepancy vector of the observations. The weights are typically set to unity for all the grey level observation equations.

In the current implementation, the geometric constraint observation equations are introduced by means of epipolar line equations or by the more generalized polynomial equation:

$$t_k = a_n(x+dx)^n + a_{n-1}(x+dx)^{n-1} + ... + a_1(x+dx) + a_0$$
$$- (y+dy) \qquad (3)$$

where a_n,... a_0 the polynomial parameters, *(x,y)* the approximate pixel coordinates of the point in the search image, *(dx, dy)* the unknown shifts and t_k the discrepancy vector.

Compared to collinearity equations, epipolar polynomial equations are simpler to implement and can be applied to images with restricted access to their sensor model information. An approximation of height Z and an alteration factor DZ is required to derive the polynomial equation. The point on the template is projected on different height planes and the trajectory of epipolar points on the search image is determined by least squares fit of a curve. The main reason for the generalization from epipolar lines to epipolar curves, modeled by polynomials, is the extension of LSM to images, with nonframe geometry, e.g. acquired from airborne linear sensors, like the ADS40 (Fricker et al., 2000). For ADS40, trajectories of epipolar points on raw imagery follow irregular and random forms due to the unpredictable motions of the aircraft, and they can not be modeled by a

line (Pateraki and Baltsavias, 2003). On the contrary, for space-borne linear sensors due to the smooth orbit trajectory the epipolar lines can be approximated locally by a line (Baltsavias and Stallmann, 1992). An alternative to the use of higher degree polynomials is to use less strict weights for the epipolar line constraints (e.g. s = 0.5 –2 pixels). The epipolar constraint approach can be also used for ADS40 L1 images, i.e. images rectified on a plane with a user-defined average height. Such images are investigated below.

2.2 Problem Statement

Some characteristics of LSM have been mentioned in Section 1. Here, we will deal with surface discontinuities and edges. If the match points lie along edges, scales are often non-determinable and estimation of the shifts is uncertain, namely in the direction of the edge, however the shift across the edge may be precise. Even if the shaping parameters are weakly determinable, the final position may often lie close to the true position if the match points are selected along the edge, especially if geometrical constraints are enforced and the edges have a sufficiently large angle with the epipolar line. This is however not guaranteed if the approximations are poor and the patch size is small, especially in the presence of different grey values due to occlusions (Fig.1).
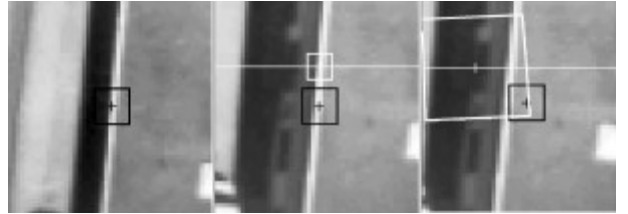

Figure 1. Example of correct (middle) and wrong (right) solution, depending on the approximate values. The template (left) is selected in the Nadir view of ADS40 L1 and the patch in the Backward view. Initial and final position of the patch is indicated with the black and white rectangle respectively. The thin white horizontal line is the epipolar line.

In the case of surface discontinuities, these will either lead to occlusions or large perspective differences. With larger bases between sensor stations higher accuracy can be achieved (better ray intersection), however, occlusions will increase. The solution to this problem is to use more than 2 images, exclude occluded rays and compute the object point from the remaining rays. ADS40 facilitates object point determination due to the quasi parallel projection in flight direction (less perspective distortions) and through the simultaneous use of 3 or more line CCDs of different viewing angles, i.e. the Nadir, Backward, Forward and possibly a spectral line, e.g. Green. In case of large perspective differences, scales and shears will be considerably different than 1 and 0 respectively and LSM will often not converge. Increasing the patch size helps convergence but then discontinuities are increasingly smoothed.

Up to now, to reduce the problems faced at discontinuities our standard multiphoto geometrically constrained matching algorithm has been used along edgels nonparallel to the epipolar lines, with small patch size (e.g. $9^2 – 11^2$ pixels), two shifts and a rotation only, and using gradients instead of grey values. The small patch size reduces discontinuity smoothing and the danger of including in the patch varying grey values due to occlusions. Use of gradients, eliminates the problem of homogeneous surfaces varying due to occlusions (e.g. in one image a black roof

shadow is visible, in another a bright vertical wall). However, the small patch size may lead to instabilities in the determination of the shifts and rotation, while the matching approximations must be very good. The matched edgels must be very dense along the discontinuity to model it nicely, while edgels parallel to the epipolar line can not be matched due to multiple solutions.

Some possible solutions to the above mentioned problems are investigated below through the use of edgels and edges and modifications of LSM. The edgel approach is similar to the one described above, but with a pre-rotation of each patch to be approximately aligned with the template. This improves approximations, stabilises the least squares solution, speeds up convergence and computing time. In addition, the template patch is rotated and made a thin rectangle, so that in case of a straight edge, only this is included in matching and not the flanking regions, which may be partially occluded, thus increasing the success rate and accuracy and leading to less smoothing. The edge approach is quite different than the approach used up to now and is described in Section 2.4. For these initial tests of the developed methods, 20 characteristic roof points covering different problem cases have been manually selected. In all cases, the epipolar constraints were used and the affine transformation of LSM was replaced by a conformal one, due to poor determinability of the affine parameters at edge points.

2.3 Edgel Matching

Matching is applied to edge pixels which are extracted in the template image beforehand by the Canny operator (Canny, 1986) or the gradient thresholding (in-house operator), or by manual selection (e.g. in case of semi-automated measurements for building roof reconstruction). Edges extracted with the Canny operator or the gradient thresholding have width of one pixel or more, respectively, and these edgels of the template image should be matched in the other images.

To derive initial approximations for the rotation, a signal analysis in the template and each patch is made. The signal ellipse is computed in a window centered at the template point and for each patch at the position after the first iteration of LSM with geometric constraints, i.e. on the epipolar line and at an improved approximate position. For edges, the signal ellipse is elongated with the major axis in edge direction. The ellipse measures, size of semi-major (q_a) and semi-minor (q_b) axes, angle (phi) between x direction and the semi-major axis and eccentricity (e) of the signal ellipse are computed according to:

$$q_a{}^2 = \frac{(\sum gxx + \sum gyy)}{2} + \sqrt{\frac{(\sum gxx - \sum gyy)^2}{4} + \sum gxy^2}$$

$$q_b{}^2 = \frac{(\sum gxx + \sum gyy)}{2} - \sqrt{\frac{(\sum gxx - \sum gyy)^2}{4} + \sum gxy^2} \tag{4}$$

$$phi = 0.5 \cdot \text{atan2}\,(2 \cdot \sum gxy, \sum gxx - \sum gyy)$$

$$e = \sqrt{1 - \frac{q_b{}^2}{q_a{}^2}}$$

where $\sum gxx$, $\sum gyy$ and $\sum gxy$ are the sums of the x- and y-gradient products in the window.

If the approximation for one of the patches is poor (e.g. far away from the edge), then the signal ellipse may not be elongated and the procedure below is interrupted. Otherwise, the pre-rotation of each patch is determined by the difference of the angle phi between patch and template. Determination of phi may be wrong, especially if the patch is large and contains edges in other directions (see Fig. 2, middle). To reduce this problem, smaller patches (e.g. 9^2 - 11^2) are justified. An example with and without pre-rotation is shown in Fig. 3(a). The seemingly wrong pre-rotation in the right image of Fig. 3(a) is just a visualisation problem. The signal ellipse and phi were not determined at the black rectangle shown, but at the result of the first iteration on the epipolar line. At this position, the edge was only partially included in the patch, being otherwise homogeneous, and thus the estimation of phi was not reliable. This problem stresses the necessity of good shift approximations before computing the signal ellipse. Furthermore, use of gradients instead of grey values has been tested. This often improves the success rate, see an example in Fig. 3(b).
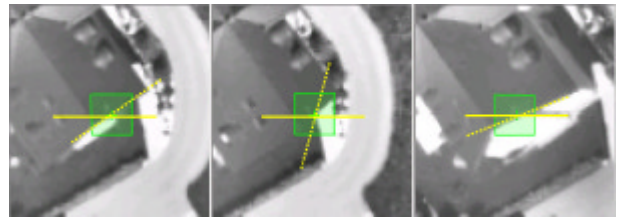

Figure 2. Selection of large patches (17 x17) on edge discontinuities. Left: template (Nadir), middle: Backward, right: Forward. The dotted line indicates the direction of the phi angle with respect to x-axis (horizontal line).
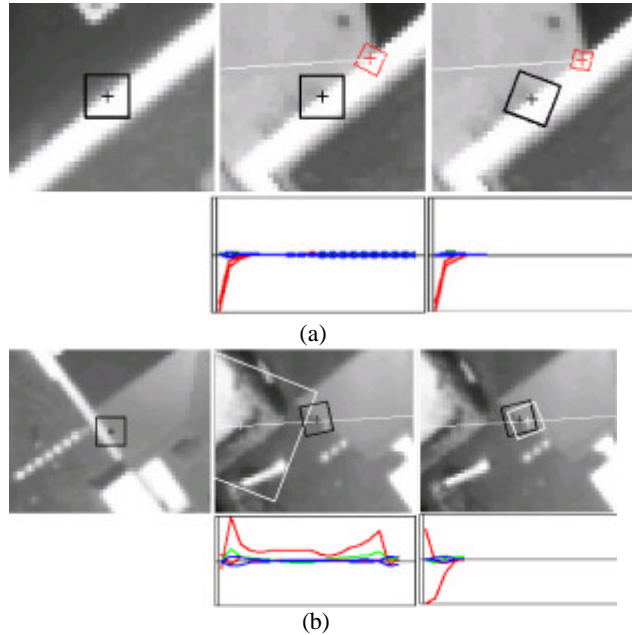

(a)

(b)

Figure 3. On the left, the selected template (9 x 9) in Nadir view, in the middle and on the right the solution the Backward view. (a) without and with pre-rotation; (b) with pre-rotation but in the middle using grey values and on the right using gradients. Initial (black) and final (grey in (a), white in (b)) position and shaping of the patch are shown. At the lower part of (a) and (b), the alterations of shaping parameters are shown.

For ADS40 L1 images the rotation, scales and shears between the images are small, since the images are rectified. In spite of that, pre-rotation with gradients compared to matching without these two options, and using the 20 test points, led to 3 times less iterations, decrease of oscillations for scales and especially shears (compare bottom of Fig. 3(a)) and increase of the success rate by 35%. Figure 2 (and also Fig. 5) shows well also the quite large perspective differences between the template images (usually selected from the Nadir line CCD) and the images from the Forward CCD with an angle of 28° to the Nadir, while the Backward CCD with 14° angle to the Nadir has less differences to the Nadir images.

To include in matching only a narrow region across the edge, the following procedure is followed. For the template, a thin rectangular patch is used and the long dimension is aligned with the edge direction. The direction of the long patch dimension is computed from the value of phi from the signal analysis of the template. The patch dimension across the patch can either be selected small for all edges (e.g. 5 pixels) or can be estimated from the analysis of the grey level ramp for each edge. The patches have the same dimensions as the template patch and are pre-rotated with respect to this new template patch orientation, again using the phi values of patch and template. The reshaping and rotation of template (and the patches) occurs before the iterations of LSM start, while the pre-rotation of the patch to fit to the template is estimated after the first iteration, as mentioned above. Fig. 4 (a) shows an example of pre-rotation with wrong matching for the Backward channel, while in Fig. 4 (b) also a template reshaping is included. Tests with the 20 points showed that false matching could be almost eliminated, as long as the derived edge directions in template and patch are reliable.

In all above procedures, the angle phi could be also estimated from the orientation of the edgels, e.g. from Canny. This may have the advantage that small gradients (e.g. noise) do not influence the computation of phi, as in Eq. (4).
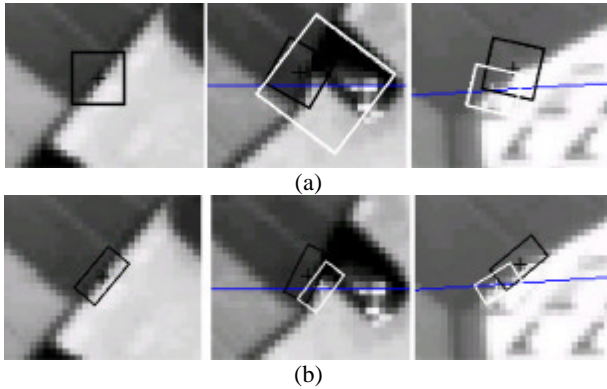

(a)

(b)

Figure 4. LSM with pre-rotation of patch (a) and with reshaping of template and patch (b). Left: template, middle: Backward, right: Forward. The initial patch and position is shown in black and the final one in white.

2.4 Edge Matching

An alternative approach to edgel matching is to use the full edge length. A feature-based approach of LSM is utilized. Single extracted edgels (one-pixel wide edges, i.e. extracted with Canny) are linked into edges. The edgel aggregation is a sequential process, where the significant edges are aggregated before the weaker ones (Henricsson, 1996) and small gaps are bridged based on criteria of proximity and collinearity. The generated edge graph is post-processed based on defined attributes in or-

der to remove weak edges and fit to the edgels straight edge segments, as long as possible. The attributes can be geometrical (e.g. length and curvature of edge), radiometrical (e.g. strength of edge) or topological (e.g. adjacency, common end points). Edges are extracted only in the template image and for each edge to be matched the patch dimension of the template is expanded in order to contain the edge points and the end points (vertices) of the edge (see left patch in Figure 5 (a), (b), (c), (d), (e)). The patch is centered at the middle point of the edge and initial approximations of the shifts, scales and shears are set to 0, 1 and 0, respectively. In addition, a different weighting scheme is used. For all grey level observation equations that correspond to edge pixels, weights are set to 1.0 and for the remaining equations weights are smaller (0.1). Thus, the contribution of off-the-edge pixels in the least squares solution is reduced. The patch should be large enough (e.g. more than 5 x 5) to avoid singularities of the system, as the number of observations should be larger the number of unknowns and the smaller weights must not be zero, especially for short edge lengths (and thus small patch sizes).

After matching the edge middle point, other edge points in the template image are selected with a step of 1 pixel. For these pixels, approximations in the patch are derived from the conformal transformation computed between patch and template for the edge middle point. The quality of these approximations depend on (a) the change of height (parallax) along the edge, and (b) the accuracy of the conformal parameters. The further the edge point is from the middle point, the higher the influence of these two factors and the worse in general the approximations. In Fig. 5 in (b) and (c), the dotted edge lines show these approximations. In (c) it is well visible that approximations are poorer for points far away from the middle point. Matching continues for the edge points, except the middle one, as follows. The edge is divided by two, and each edge segment is treated as the whole edge above, i.e. the template patch includes the edge segment end points and matching is performed. However, in this case quite good approximations exist for the shifts, derived from the matching of the whole edge. This continues by dividing each segment in two and so on and so forth, until the edge segments become less than 11 pixels long. At this stage no matching has been performed yet for the two end points of the original edge, but approximations exist from the matching of the middle points of the two outer edge segments. For matching the end points, square patches (9x9 pixels) are used. Before adopting the result as correct, the convergence and the change of the matching solution found from the initial approximation are checked. If the edge end points are end points for more than one edge, then the approximation for matching the end points are derived from the average of the approximation from each edge. Thus, common end points of edges get one common height and the edges are connected in 3D space.

This approach proved relative robust, with fast convergence (3-7 iterations), and due to the often large patch size, requires less good approximations than conventional LSM, reduces the danger of multiple solutions and leads to a safer determination of rotation. Even the case of edges parallel to the epipolar line could be partially treated, when at one of the end points of the edge (that are included in the template patch), other edges with a large enough angle to the epipolar line were included, i.e. corners on roof tops (Fig. 6). However, the problem of edges parallel to the epipolar lines is not generally solved. Furthermore, occlusions may still cause false matching, or even if matching is correct, they may cause wrong scale and rotation estimation in the conformal transformation, and thus wrong approximations for the remaining edge points to be matched.
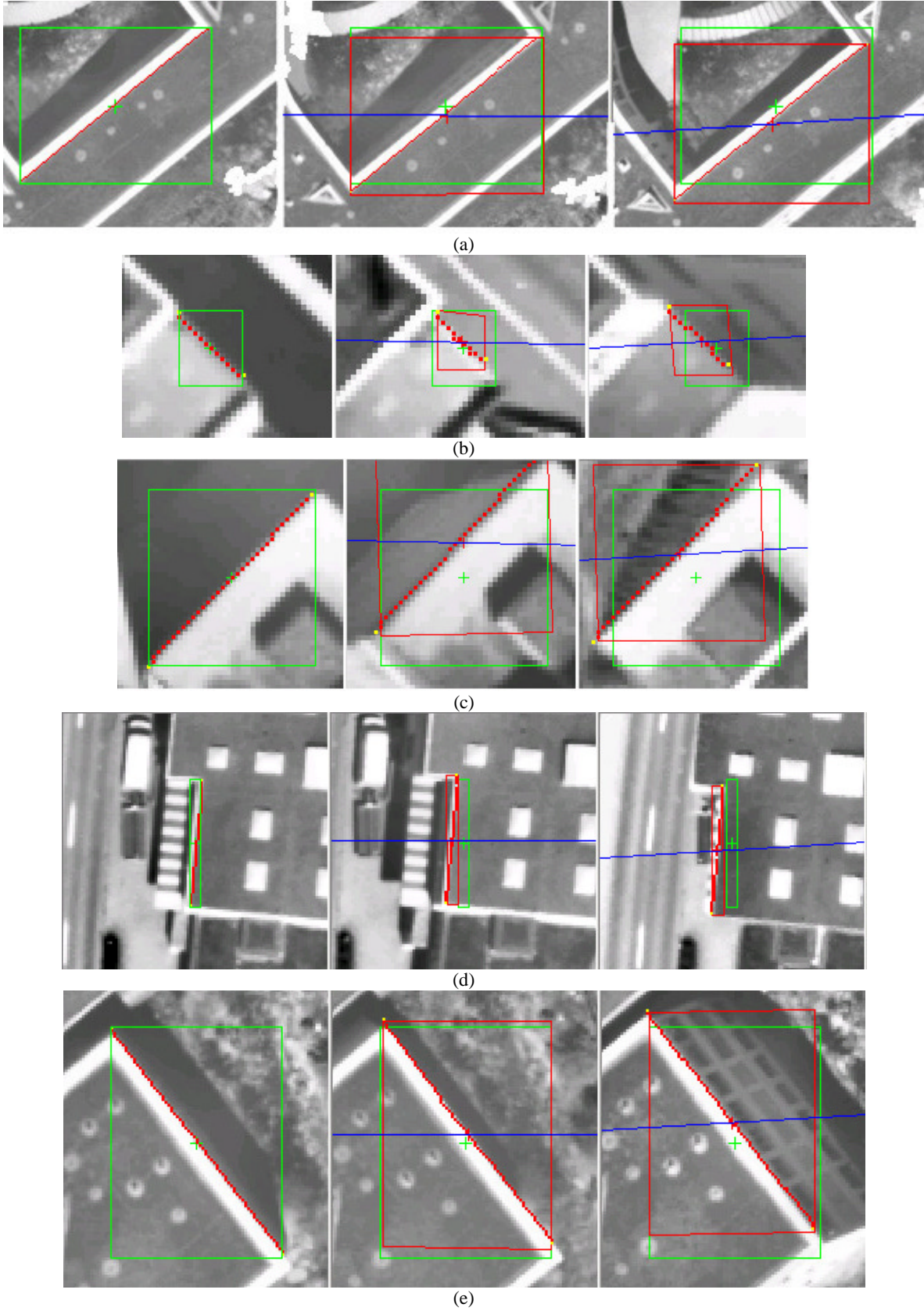
Figure 5. Examples of edge LSM. Edges are extracted in the template image (left) and matched in the remaining images (middle, right). Convergence of the least squares solution is achieved in 3 to 7 iterations. The dots indicate the edge points. Results are illustrated after the LSM solution for the middle of the edge. The light and dark grey rectangles show the initial and final patches respectively.
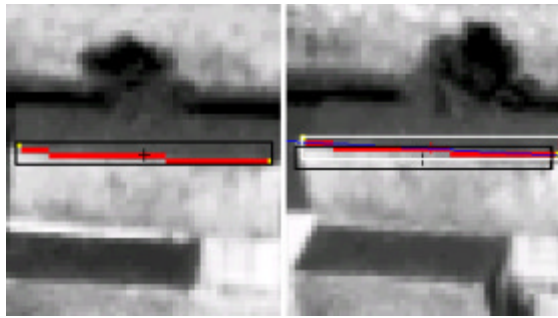
(a)

Figure 6. LSM for edges parallel to epipolar lines. Initial (black), final (white) position and matched edge are shown.

The edge method could be combined with preshaping of the template as described in Section 2.3, in order to save computation time. However, execution speed is not, at this stage of investigations, the major concern, plus the method of excluding or reducing the influence of pixels in the patch through appropriate weights is general, flexible and elegant.

3. CONCLUSIONS

Various modifications of LSM, for improving its performance at surface discontinuities, have been presented and evaluated. In particular, these methods adapt the template patch orientation and dimensions, improve the approximations for the rotation and shift of the patches, decrease the influence of off-edge pixels and reduce multiple solutions for edges parallel to the epipolar lines. These measures lead to less discontinuity smoothing and increase the success rate and accuracy. The methods should be improved and refined, and also extended to better handle still unsolved problems, e.g. partially occluded edges. After these developments, extensive tests over large areas with manually measured DSMs (incl. building roofs) are planned.

REFERENCES

Ackermann, F., 1984. High Precision Digital image Correlation. In: Photogrammetric Week, No. 9, Institute for Photogrammetry, University Stuttgart.

Baltsavias, E.P., 1991. Multiphoto geometrically constrained matching. Ph.D. Thesis, Institute of Geodesy and Photogrammetry, ETH Zurich, Report No. 49, 221 p.

Baltsavias, E.P., Stallmann D., 1992. Advancement in matching of SPOT images by integration of sensor geometry and treatment of radiometric differences. In: IAPRS, Vol. 29, Part B4, pp. 916-924.

Canny, J., 1986. A computational approach to edge detection. IEEE Transactions on Pattern Analysis and Machine Intelligence 8 (6), 679-698.

Ebner, H., Heipke, C., 1988.Integration of digital image analysis and object surface reconstruction. In: IAPRS, Vol. 27, Part B11, pp. III: 534-545.

Foerstner, W., 1982. On the Geometric Precision of Digital Correlation. In: IAPRS, Vol. 24, Part 3, pp. 176-189.

Fricker, P., Sandau, R., Walker, A.S., 2000. Development of an airborne digital sensor for photogrammetric and remote sensing applications. Proc. ASPRS Annual Conference, Washington DC, USA (on CD-ROM).

Gruen, A., 1985. Adaptive least squares correlation: A powerfull image matching technique. South African Journal of Photogrammetry, Remote Sensing and Cartography 14 (3), 175-187.

Gruen, A., Baltsavias, E.P., 1988. Geometrically Constrained Multiphoto Matching. PERS 54(5), 633-641.

Gruen, A., Stallmann, D., 1992. High accuracy matching of object edges. Proc. SPIE, "Videometrics", Vol. 1820, pp. 70-82.

Gruen, A., Agouris, P., 1994. Liner feature extraction by least squares template matching constrained by internal shape forces. In: IAPRS, Vol. 30, Part3, pp. 316-323.

Helava, U.V., 1988. Object-space least-squares correlation. PERS 54 (6), 711-714.

Henricsson, O., 1996. Analysis of Image Structure using Color Attributes and Similarity Relations. Ph.D. Thesis, Institute of Geodesy and Photogrammetry, ETH Zurich, Report No.59.

Krupnik, A., Schenk, T., 1997. Experiences with matching in the object for aeriotriangulation. ISPRS Journal of Photogrammetry and Remote Sensing 52 (4), 160-168.

Li, M.X., 1989. Hierarchical multi-point matching with simultaneous detection and location of breaklines. Ph.D. thesis, Royal Institute of Technology, Department of Photogrammetry.

Pateraki, M., Baltsavias, E., 2003. Analysis and Performance of the Adaptive Multi-image matching Algorithm for Airborne Digital Sensor ADS40. Proc. ASPRS Annual Conference, Anchorage, AK, USA, 5-9 May (on CD-ROM).

Rosenholm, D., 1986. Accuracy improvement in digital matching. Photogrammetric Reports No. 52, Transactions of the Royal Institute of Technology, Department of Photogrammetry, Stockholm, Sweden.

Rosenholm, D., 1987. Multi-point matching using least squares technique for evaluation of three-dimensional models. PERS 53 (6), 621-626.

Schenk, T., Li J.-C., Toth, C., 1990. Hierarchical approach to reconstruct surfaces by using iteratively rectified imagery. In: IAPRS, Vol. 28, Part 5/1, pp. 464-470.

Tseng, Y.-H., Schenk, T., 1992. A least squares approach to matching lines with Fourier descriptors. In: IAPRS, Vol. 29, Part B3, pp. 469-475.

Wrobel, B.P., 1991. Least-squares methods for surface reconstruction from images. ISPRS Journal of Photogrammetry and Remote Sensing 46 (2), 67-84.